

## Equilibrium, kinetic and thermodynamic studies of Na<sup>+</sup> adsorption from aqueous solutions on homo-ionized K- and NH<sub>4</sub>-kaolin

H.S. Ali<sup>(1)</sup>, K. S. Abou-El-Sherbini<sup>(2)</sup>, O.A. El-Gammal<sup>(3)</sup> and N.I.Talha<sup>(1)</sup>

<sup>(1)</sup>Soils, water and environment research institute, Agriculture Research Centre, Egypt.

<sup>(2)</sup>Department of Inorganic Chemistry, National Research Centre, 33 El Bohouth st. (former Eltahrir st.), P.O. 12622, Dokki, Giza, Egypt.

<sup>(3)</sup>Department of Chemistry, Faculty of Science, Mansoura University, (2), P.O.Box 70, Mansoura- Egypt

Received: 20/7/2020  
Accepted: 12/8/2020

**Abstract:** Egyptian kaolin clay (UnK) was homo-ionized with K<sup>+</sup> and NH<sub>4</sub><sup>+</sup> to obtain K-K and N-K, respectively. The analysis of the molar leaching solutions of KCl, NH<sub>4</sub>Cl or HCl revealed an original cation exchange capacity of UnK up to 6.08 meq per 100 g. The adsorption parameters of Na<sup>+</sup> on K-K and N-K were examined in aqueous solutions. The equilibrium adsorption data were evaluated using Langmuir, Freundlich adsorption and Dubinin–Radushkevich–Kaganer isotherm models. Freundlich model was the best that described the adsorption process and the maximum capacities ( $q_{\max}$ ) are found to be enhanced to 75.6 and 17.5 mg g<sup>-1</sup>, respectively. The experimental data fitted well the pseudo-second-order kinetics model. The thermodynamic parameters such as standard Gibbs free energy ( $\Delta G^{\text{ads}}$ ), enthalpy ( $\Delta H^{\text{ads}}$ ) and entropy changes ( $\Delta S^{\text{ads}}$ ) for the adsorption process were calculated. The negative values of the Gibbs free energy confirm that the adsorption processes are spontaneous and thermodynamically favorable while the negative value of  $\Delta H^{\text{ads}}$  supports the exothermic physicochemisorption of the adsorption process. Both homo-ionized kaolin samples are promising cheap adsorbents for lowering the sodicity of soil while gradually exchanging valuable nutrients for plants.

**keywords:** Na<sup>+</sup>; Adsorption equilibrium; Kaolin; Thermodynamics; Kinetics

### 1. Introduction

Salt-affected soils are found in arid and semi-arid climates in more than one hundred countries of the world, especially Egypt, where many regions are also affected by irrigation-induced salinization<sup>[1]</sup>. This problem shall upsurge in the future by increasing the use of pretreated waste water in irrigation. Salinity becomes a problem when the total amount of salts which accumulate in the root zone is high enough to negatively affect plant growth depending on its type.

Due to the accumulation of salt, water uptake by plant roots in the soil become difficult thus disturbing water balance, while high concentrations of salts in plant tissue were found to be toxic.

Sodicity refers to the sodium content of the irrigation water. Because of the relatively large size, single electrical charge, and hydration status of the sodium ion it

particularly can cause soil dispersion. Sodic soil conditions make it difficult for plants to become established, for roots to penetrate the soil, and for plants to receive sufficient nutrients and water. Overall, those effects have negative impacts on plant yield and survival<sup>[2]</sup>. A soil is classified as sodic if exchangeable sodium percentage (ESP) exceeds 15%<sup>[3]</sup>. Hence, it should be reduced below this percentage.

Nowadays, many desalination technologies are in use to produce freshwater from saline water. Electro-dialysis, vapor compression, multi-stage flash distillation, multiple-effect distillation, and reverse osmosis distillation have become standard desalination technology in the world at a recent decade<sup>[4]</sup>. Indeed, these technologies can produce large amounts of freshwater but they are costly and cannot target sodium selectively.

Due to low operational costs as well as its friendly aspects to environment, desalination using sorbent material is considered as eco-desalination technique<sup>[5]</sup>. Unwanted species are selectively sorbed by manipulating suitable sorbent materials in this process. Low cost, chemical and mechanical stability, and high cation exchange capacity are necessary requirements that are common characteristic of clay minerals<sup>[6]</sup>. The clay minerals such as kaolin, bentonite and montmorillonite are widely abundant worldwide with low prices and acceptable quality. Kaolin, in particular, is found in northern Eastern desert (Egypt)<sup>[7]</sup>. The liquid limits of clays rich in smectite decreased with the NaCl concentrations, while those of the kaolinite were relatively stable<sup>[8]</sup>. It also acquires a hydrophilic rigid two dimensional inorganic structure that is an advantage compared with the common organic ion exchangers.

Kaolinite, the major mineral of kaolin, is abundant in soils and sediments and is capable of interacting with other elements of soil for mechanical stability of the soil column. The ideal formula of kaolinite is  $\text{Al}_2\text{Si}_2\text{O}_5(\text{OH})_4$ <sup>[9]</sup>. Its structure is composed of the 1:1 type and consists of alternating sheets of tetrahedral silica and octahedral alumina<sup>[9b]</sup>. This structure is well balanced, with little or no ionic substitution and therefore low cation exchange capacity. Its ion-exchange capacity ranges between 3 and 15 meq/100g<sup>[10]</sup>. The adsorption capacity of kaolinite is depending on its outer surface and edges.

Reduction of water salinity was reported with many sorbents such as zeolite, which was successfully reported<sup>[11]</sup>. Bentonite membranes were also used for the removal of salinity reduction of waste water<sup>[12]</sup>. Natural and acid-activated kaolin were confirmed to have monolayer adsorption capacities of 23.8 and 34.5 mg g<sup>-1</sup>, respectively<sup>[13]</sup>. These modified clays, in near-homoionic form, have a higher CEC because the new counter ion is more easier to exchange<sup>[14]</sup>. To the best of our knowledge, kaolin was not yet examined for water sodicity reduction despite it is a common component of different soils. Herein, kaolin is homo-ionized with K<sup>+</sup> or NH<sub>4</sub><sup>+</sup> as important nutrients for plants and less hazardous to them compared with Na<sup>+</sup>. The ion exchange

characteristics of the modified kaolin samples are also studied in respect to Na<sup>+</sup> removal in a batch-mode of separation.

## 2. Experimental

### 2.1. Materials

Egyptian kaolin rock was kindly provided from Prof. Dr. Adel Akarish, National Research Centre, and Cairo, Egypt. The raw Egyptian kaolin sample was from South Sinai, and has been previously described<sup>[13]</sup>. Potassium chloride was from El-Gomhouria Company For Drugs, Egypt. Other chemicals were from Sigma- Aldrich, USA or Sigma- Aldrich, USA. Aqueous standard solutions of the required compounds were prepared by dissolving the required salt in distilled water.

### 2.2. Instruments

Flame Atomic Absorption Spectrometer (FAAS) model 3300 from Perkin Elmer, USA, was used for elemental analysis of Na and K ions. A pH-meter from pH meter (WPA Linton, Cambridge, UK), was used for pH measurements.

### 2.3. Methods

#### 2.3.1. Homo-ionization technique

The raw kaolin was ball-milled and the -112 micron portion (50%) was sieved and coded UnK. It was pretreated to replace exchangeable ions with useful ions for plant growth that may reduce sodicity of the irrigation water while they are released from the homo-ionized kaolin to the aqueous phase. A mass (m) of 10 g of UnK was mixed with a volume (V) of 100 mL of aqueous 1M KCl solution then the suspension was shaken for 48 h, then centrifuged. The supernatant solution was discarded and stored for metal analysis. Another fresh 100 mL of aqueous 1M KCl solution was added to the centrifuged kaolin and the saturation step was repeated four times. The final centrifuged kaolin was washed with DW till chloride free filtrate using AgNO<sub>3</sub> test, then the K-homo-ionized kaolin was dried at 70°C till constant mass. The product was coded K-K. The same homo-ionization procedure was repeated replacing 1M KCl with 1M NH<sub>4</sub>Cl, adjusted at pH 7.0 using ammonia solution, to obtain ammonium-homo-ionized kaolin (N-K). The released Na, K, Ca and Mg ions in the supernatant liquors for each batch were

determined. The concentration ( $C$ ,  $\text{mg L}^{-1}$ ) of  $\text{Na}^+$  and  $\text{K}^+$ , were determined by FAAS whereas  $\text{Mg}^{2+}$  and  $\text{Ca}^{2+}$  were determined by complexometric titration with 0.01M EDTA<sup>[15]</sup>. The released metal content ( $M$ ,  $\text{mg g}^{-1}$ ) was calculated by:

$$M = \frac{C(\text{mg L}^{-1}) \cdot V(\text{L})}{m(\text{g})} \text{mg g}^{-1} \quad (1)$$

Cation exchange capacity (CEC, meq per 100 g) was calculated for the leached Na, K, Ca and Mg ions using 1M KCl or  $\text{NH}_4\text{Cl}$  by Eq (2):

$$\text{CEC} = \sum \frac{M \text{ of the metal ion}}{\text{atomic mass}} \cdot 100 \quad (2)$$

### 2.3.2. Adsorption studies

For the analysis of HCl-leachable elements, 0.2 g of the kaolin samples were shaken in 100mL 1M HCl at 50°C for 24 h, then the suspensions were filtered. The metal content ( $M$ ,  $\text{mg g}^{-1}$ ) was determined and calculated as described above by Eq(1).

### 2.3.3. Effect of initial concentrations

The effect of initial concentrations ( $C_0$ ) was studied at room temperature by adding 0.1 g of each adsorbent with 20 mL of 10-500  $\text{mg L}^{-1}$  of  $\text{Na}^+$  aqueous solutions as NaCl. Then, the suspensions were shaken for six h and left for equilibration for seven days. The suspensions were centrifuged and the equilibrium concentrations of Na ( $C_e$ ) in the supernatant liquors were determined by FAAS.

### 2.3.4. Effect of contact time

To study the effect of time of shaking, 0.1 g of each adsorbent was suspended in 20 mL of initial concentration 100  $\text{mg L}^{-1}$  of  $\text{Na}^+$  aqueous solutions at room temperature. The suspensions were shaken for the time intervals 5, 10-1440 min. Then, the suspensions were centrifuged and final concentrations of Na ( $C_f$ ) in the separated liquors were determined by FAAS

### 2.3.5. Effect of temperature

A mass of 0.1 g of each adsorbent was added to 20 mL of  $\text{Na}^+$  solution with initial concentrations of 50, 100 or 200  $\text{mg L}^{-1}$  of  $\text{Na}^+$ . Then the suspension was shaken for 24h while keeping temperature at 20, 40, or 60°C. The suspensions were centrifuged and the residual  $\text{Na}^+$  concentrations in the separated liquors were measured by FAAS.

## 2.3.6. Mathematical calculations

### 2.3.6.1. Adsorption isotherm model fitting

The experimental data were fitted by the adsorption isotherms models of Langmuir<sup>[16]</sup> and Freundlich<sup>[17]</sup>. The linear Langmuir isotherm equation can be expressed by Eq. 3:

$$\frac{C_e}{q_e} = \frac{1}{K_L q_{\max}} + \frac{1}{q_{\max}} C_e \quad (3)$$

Where  $C_e$  is the equilibrium concentration in solution ( $\text{mg L}^{-1}$ ),  $q_e$  is the Na amount adsorbed per unit mass of adsorbent at equilibrium ( $\text{mg g}^{-1}$ ),  $q_{\max}$  is the maximum adsorption capacity at monolayer coverage ( $\text{mg g}^{-1}$ ) and  $K_L$  the Langmuir constant related to adsorption energy ( $\text{Lmg}^{-1}$ ). The equilibrium adsorption capacity,  $q_e$  was calculated by the equation:

$$q_e = \frac{V(C_0 - C_e)}{m} \quad (4)$$

The maximum adsorption capacity and Langmuir constant were calculated from the slope and intercept of the linear plots of  $C_e/q_e$  versus  $C_e$  to determine the value of  $q_{\max}$  and  $b$ , which gives a straight line of slope  $1/q_{\max}$ , corresponding to a complete monolayer coverage ( $\text{mg g}^{-1}$ ) and the intercept is  $1/(K_L q_{\max})$ .

The essential characteristics and the feasibility of the Langmuir isotherm can be expressed in terms of a dimensionless equilibrium factor  $R_L$  that is given by Eq. (5):

$$R_L = \frac{1}{1 + C_0 K_L} \quad (5)$$

The linear form of the Freundlich equation is given by Eq. (6):

$$\ln q_e = \ln K_F + \frac{1}{n} \ln C_e \quad (6)$$

where,  $K_F$  ( $\text{dm}^3 \text{g}^{-1}$ ) and  $n$  are Freundlich adsorption isotherm constants, related to the adsorption capacity and adsorption intensity respectively. The plot of  $\ln q_e$  versus  $\ln C_e$  was used to generate the intercept value of  $K_F$  and the slope  $1/n$ .

The Dubinin–Radushkevich–Kaganer isotherm is given by<sup>[18]</sup>:

$$\ln q_e = \ln q_m - K_{D-R} \varepsilon^2 \quad (7)$$

where  $\varepsilon$  is Polanyi potential, and is given by  $\varepsilon = RT \ln (1 + 1/C_e)$ ,  $q_m$  is the theoretical adsorption capacity,  $T$  is the absolute temperature in Kelvin,  $R$  is the universal gas constant,  $8.314 \text{ (J mol}^{-1} \text{ K}^{-1})$  and  $K_{D-R}$  is the constant related to the adsorption energy. The mean free energy of adsorption ( $E$ ) was calculated from the constant  $K_{D-R}$  using the relation.

$$E = \sqrt{\frac{1}{2K_{D-R}}} \quad (8)$$

### 2.3.6.2. Thermodynamic Parameters

The Gibb's free energy of adsorption of  $\text{Na}^+$  ( $\Delta G^{\text{ads}}$ ,  $\text{kJ mol}^{-1}$ ) on the adsorbents was calculated directly from the van't Hoff isochore Eq. (9).

$$\Delta G^{\text{ads}} = -RT \ln K^{\text{ads}} \quad (9)$$

Where  $K^{\text{ads}}$  is the thermodynamic equilibrium constant of adsorption,  $T$  is the absolute temperature and  $R$  is the molar gas constant ( $8.314 \text{ J mol}^{-1} \text{ K}^{-1}$ ). For a dilute solution of charged adsorbate, the thermodynamic equilibrium constant of adsorption can be reasonably replaced by the Langmuir equilibrium constant ( $K_L$ ,  $\text{L mole}^{-1}$ )<sup>[19]</sup>. Accordingly, Eq. (9) will be rewritten to be:

$$\Delta G^{\text{ads}} = -RT \ln K_L^{\text{ads}} \quad (10)$$

As  $\Delta G^{\text{ads}}$  is correlated with the changes of enthalpy ( $\Delta H^{\text{ads}}$ ) and entropy ( $\Delta S^{\text{ads}}$ ) by Eq. (11):

$$\Delta G^{\text{ads}} = \Delta H^{\text{ads}} - T \Delta S^{\text{ads}} \quad (11)$$

$\Delta H^{\text{ads}}$  and  $\Delta S^{\text{ads}}$  can be obtained by plotting  $\Delta G^{\text{ads}}$  (y axis) against  $T$  (x axis) where the resulting linear correlation has a slope representing  $-\Delta S^{\text{ads}}$  and an intercept with the y axis equals  $\Delta H^{\text{ads}}$ .

### 2.3.6.3. Fitting of kinetic models

To study the adsorption kinetics of  $\text{Na}^+$  on the adsorbents, the experimental data were examined by the pseudo-first-order

and pseudo-second-order kinetic models<sup>[20]</sup>.

Pseudo 1<sup>st</sup> order model is expressed as shown in Eq.12:

$$\ln(q_e - q_t) = \ln q_e - K_1 t \quad (12)$$

Pseudo 2<sup>nd</sup> order model is expressed as shown in Eq (13):

$$\frac{t}{q_t} = \frac{1}{K_2 q_e^2} + \frac{1}{q_e} t \quad (13)$$

Where  $k_1$  is the rate constant of the pseudo 1<sup>st</sup> order adsorption ( $\text{min}^{-1}$ ),  $k_2$  is the rate constant of the pseudo 2<sup>nd</sup> order adsorption ( $\text{g mg}^{-1} \text{ min}^{-1}$ ), and  $q_e$  and  $q_t$  represent the amount of  $\text{Na}^+$  adsorbed ( $\text{mg g}^{-1}$ ) at equilibrium and at time  $t$ , respectively. By plotting  $t/q_t$  versus  $t$  using the pseudo 2<sup>nd</sup> order equation, the values of  $q_e$  and  $K_2$  can be calculated. Then the initial adsorption rate,  $h$  ( $\text{mg g}^{-1} \text{ min}^{-1}$ ) can be calculated according to Eq (14):

$$h = K_2 q_e^2 \quad (14)$$

The intra-particle diffusion rate model (Weber-Morris equation)<sup>[21]</sup> was fitted according to Eq.(15):

$$q_t = k_{ip} t^{1/2} + C_i \quad (15)$$

$q_t$  represents the amount of  $\text{Na}^+$  adsorbed ( $\text{mg g}^{-1}$ ) at time  $t$ ,  $K_{ip}$  is the intra-particle diffusion rate constant at an stage I, and  $t^{1/2}$  is the square root of time in minutes and  $C_i$  ( $\text{mg g}^{-1}$ ) is the intercept of the linear plot of Eq. (15).

## 3. Results and discussion

Raw Egyptian kaolin, collected from Sinai, was reported to contain constituents of  $\text{MgO}$ , 0.14%,  $\text{CaO}$ , 0.16,  $\text{Na}_2\text{O}$ , 0.07 and  $\text{K}_2\text{O}$ , 0.08% in addition to major and trace constituents<sup>[13]</sup>. The minor constituents dropped to 0.06, 0.03, 0.02, and 0.08%, respectively upon treatment with 5M HCl at 70°C. Considering this harsh conditions of treatment, the lost ions could not be assured to be ion exchangeable, carbonate or structural contents. Therefore, milder procedures were followed to define the extractable ions of UnK using 1M HCl, 1M  $\text{NH}_4\text{Cl}$  adjusted at pH 7 or 1M KCl<sup>[22]</sup>.

During the five batches of the homo-ionization process of UnK, the released  $\text{Na}^+$ ,  $\text{K}^+$ ,  $\text{Mg}^{++}$  and  $\text{Ca}^{++}$  concentrations were followed in the extracts as shown in Figure 1. The released metal ion concentrations dropped quickly at the beginning until they almost stabilized in the last two. Obviously, KCl was more powerful in releasing metal ions compared with  $\text{NH}_4\text{Cl}$ . Also, the released metal amounts followed the order  $\text{Ca} > \text{Mg} > \text{Na} > \text{K}$ .

The extracted metal ions by 1M HCl treatment account for the concomitant metal

carbonate and the exchangeable ions while those leached with  $\text{NH}_4\text{Cl}$  and  $\text{KCl}$  account for the exchangeable ions only [23]. Table (1) shows the values of leached metal ions from UnK, K-K and N-K with the applied extracting agents. Surprisingly,  $\text{KCl}$  was more effective than  $\text{NH}_4\text{Cl}$  in leaching the exchangeable ions  $\text{Na}^+$ ,  $\text{K}^+$ ,  $\text{Mg}^{++}$  and  $\text{Ca}^{++}$  on contrary to their leaching results to some heavy metal ions [23a].

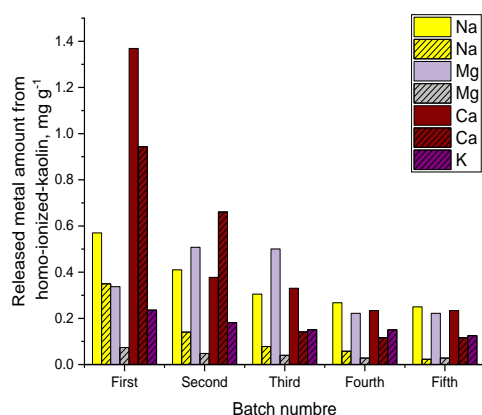


**Fig (1)** Released minor metal ions during the homo-ionization process using 1M  $\text{KCl}$  (plain) or 1M  $\text{NH}_4\text{Cl}$  (dashed).

**Table (1)** Analysis of  $\text{Na}^+$ ,  $\text{K}^+$ ,  $\text{Mg}^{++}$  and  $\text{Ca}^{++}$  in UnK and its homo-ionized products leached with 1M  $\text{NH}_4\text{Cl}$ ,  $\text{KCl}$  or  $\text{HCl}$ .

Leached ion ( $\text{mg g}^{-1}$ )	1M $\text{NH}_4\text{Cl}$	1M $\text{KCl}$	1M $\text{HCl}$		
	UnK	UnK	UnK	K-K	N-K
$\text{Na}^+$	0.65	1.80	1.47	0.59	0.25
$\text{K}^+$	0.84	-	0.65	3.03	0.475
$\text{Mg}^{++}$	0.22	1.79	27.95	23.8	18.95
$\text{Ca}^{++}$	1.98	2.54	13.20	8.8	13.2
Total released metal ion, mEq per 100 g	16.67	35.28	-		

This difference may be explained by the ability of ammonia to form soluble complexes with many metal ions, which is not possible for the investigated metal ions.

The total cation exchange capacity (CEC) including possible water soluble salts of UnK was 16.67 and 35.28 meqper gas obtained from the homo-ionization treatment with 1M  $\text{NH}_4\text{Cl}$  and  $\text{KCl}$ , respectively. Because  $\text{KCl}$  cannot be used to determine the exchangeable potassium ions, its value that was obtained from  $\text{NH}_4\text{Cl}$  was added to the CEC value obtained from  $\text{KCl}$ , and the actual total CEC of UnK for the four investigated metal ions should be modified

to be 37.5 meqper 100 g by adding the obtained released  $\text{K}^+$  value with  $\text{NH}_4\text{Cl}$  (2.15 meqper 100 g). Other possible trace metal CEC contributions may be neglected according to their low values in the elemental analysis [13].

The released metal ions from UnK by 1M  $\text{HCl}$  include the non-exchangeable metal salts such as magnesium and calcium carbonate that agrees with reported data [13]. The results of  $\text{HCl}$  leaching indicated a reduction in the contents of the investigated metals in the homo-ionized kaolin except for  $\text{K}^+$  in K-K that achieved an increase of 2.38  $\text{mg g}^{-1}$  representing a K-CEC of 6.08 meq per 100 g.

### 3.1. Adsorption studies

#### 3.1.1. Effect of initial concentration

The effect of the initial concentration on the adsorption isotherms of  $\text{Na}^+$  on K-K and N-K is shown in Figure (2). The adsorption isotherms are characteristic of type S3 according to the classification proposed for liquid-solid interactions by Giles et al. [24]. They indicate that the activation energy for desorption of the solute is concentration-dependent, and/or is markedly reduced by large negative contributions of the solvent or a second solute, which is expected for ion exchange on microporous solids. In addition, it was reported that the dielectric constant of kaolinitic sediment decreases while its equilibrium volume increases with the increase in the electrolyte concentration exposing larger surface for the ion exchange process [25].

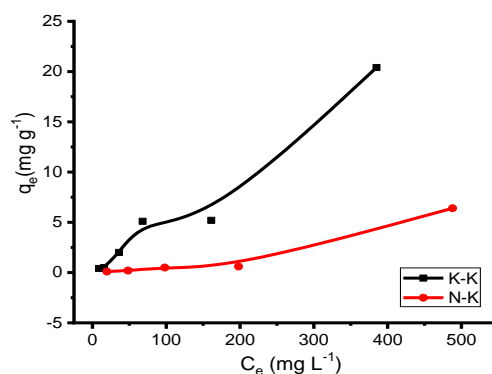


**Fig 2.** Adsorption isotherms of  $\text{Na}^+$  on K-K and N-K.

The adsorption isotherms were studied with three adsorption isotherm models, namely, the Langmuir, Freundlich and Dubinin–Radushkevich–Kaganer (DRK) models. Table

(2) summarizes the parameters of the Freundlich and DRK models whereas Langmuir model was completely excluded for inconvenience. The  $R^2$  values indicated the low fitness of the studied adsorption models for  $\text{Na}^+$  on K-K and N-K especially using Langmuir isotherm model, which may be explained in view of the ion exchange nature of the process that does not resemble an adsorption process as illustrated in Eq. (16):

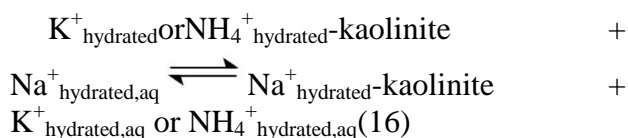


**Table 2.** Isotherm model parameters for the adsorption of  $\text{Na}^+$  on K-K and N-K.

Freundlich isotherm parameters			
Adsorbent	1/n	$K_F$ (mg/g)	$R^2$
K-K	1.069	0.034	0.956
N-K	1.302	0.001	0.922
DRK isotherm parameters			
Adsorbent	$q_{\text{max}}$ ( $\text{mg g}^{-1}$ )	E ( $\text{kJ mol}^{-1}$ )	$R^2$
K-K	75.6	5.78	0.922
N-K	17.5	5.15	0.878

However the best models that describe the adsorption of  $\text{Na}^+$  on K-K and N-K are that of Freundlich model. The values of 1/n indicate weak and unfavorable adsorption of  $\text{Na}^+$  on K-K and N-K within the studied ion concentrations.

The mean free energy, derived from DRK model, provides information about whether the mechanism of adsorption is chemical or physical process. Accordingly, the positive adsorption energies of  $E = 5.78$  and  $5.15 \text{ kJ mol}^{-1}$  obtained for  $\text{Na}^+$ , on K-K and N-K, respectively, indicate that these adsorbents are physically adsorbed. Considering the large difference in the size of the solvated exchanged ions, where  $\text{Na}^+_{\text{aq}}$  ( $5.60\text{--}7.90 \text{ \AA}$ )  $>$   $\text{K}^+_{\text{aq}}$  ( $3.80\text{--}5.32 \text{ \AA}$ ) or  $\text{NH}_4^+_{\text{aq}}$  ( $5.37 \text{ \AA}$ ) [25] the  $q_{\text{max}}$  value for N-K ( $17.5 \text{ mg g}^{-1}$ ) was expected to be smaller than that for K-K ( $75.6 \text{ mg g}^{-1} \equiv 330 \text{ mEq per 100 g}$ ) based on the limited surface covered by  $\text{K}^+_{\text{aq}}$  compared with  $\text{NH}_4^+_{\text{aq}}$ . However, the obtained Na-exchange capacities are very much higher than the K-CEC value obtained from the elemental analysis of the homo-ionization products ( $6.08 \text{ meq per 100 g} \equiv 3.49 \text{ mg g}^{-1}$ ). This indicates the noticeable enhancement of the kaolin CEC that may be

explained by the better polarizability of the heavier and the larger size of the hydrated sodium ion compared with potassium or ammonium hydrated ions.

Comparing the adsorption capacity of  $\text{Na}^+$  on K-K to various newly reported adsorbents (Table 3), it can be concluded that K-K has a moderate capacity although it is characterized by its very cheap cost in addition to its simple treatment method and importance of the exchanged potassium to plants.

**Table 3.** Comparison between the removal capacity of  $\text{Na}^+$  using K-K and N-K with other adsorbents.

Adsorbent	$q_{\text{max}}$ ( $\text{mg g}^{-1}$ )	$t_{\text{eqmin}}$	Ref.
activated coconut coir	43.7	20	[26]
TOA	4.1	120	[27]
activated carbon	134.2		[28]
Canadian Zeolite	$5.8 \pm 0.5$	1440	[29]
Bear River Zeolite	$14.3 \pm 0.4$		
St. Cloud Zeolite	$5.6 \pm 0.7$		
amorphous carbon	135.45	60	[30]
activated zeolite	67.5%		[31]
Natural zeolite	3.7	720	[32]
$\text{NH}_4^+$ treated zeolite	8.8		
K-K	75.6	360	Present work
N-K	17.5	360	

$t_{\text{eq}}$  = equilibration time. TOA = tetraoctylammonium monensin

### 3.1.2. Effect of temperature

Figure (3) shows the effect of temperature on the adsorption isotherms of K-K (left) and N-K (right) towards  $\text{Na}^+$  at  $C_0$  50, 100 and 200  $\text{mg L}^{-1}$ . The adsorption process decreases as the temperature increases, indicating that the adsorption reaction is exothermic in nature. The obtained values  $\Delta G^{\text{ads}}$  were negative ( $-17.14$ ,  $-12.59$  and  $-13.75 \text{ kJ mol}^{-1}$  for K-K and  $-12.64$ ,  $-18.56$  and  $-10.61 \text{ kJ mol}^{-1}$  for N-K at 20, 40 and  $60^\circ\text{C}$ , respectively), suggesting the spontaneous nature of the ion exchange process and meanwhile confirming the feasibility of the ion exchange process.  $\Delta H^{\text{ads}}$  was  $-41.082$  and  $-29.817 \text{ kJ mol}^{-1}$  for K-K and N-K, respectively, which indicates that the adsorption of  $\text{Na}^+$  occurs through physicochemical exothermic processes. Negative values were obtained for  $\Delta S^{\text{ads}}$  ( $-84.91$  and  $-50.71 \text{ kJ K}^{-1} \text{ mol}^{-1}$  for K-K and N-K, respectively), indicating a decrease in the system randomness. The decrease in  $\Delta S$  is



expected in the adsorption processes considering the loss of one degree of freedom due to the transport of freely moving dissolved  $\text{Na}^+$  ions from the aqueous solution to the adsorbent phase. The inference from these results is that the endothermic adsorption is entropically driven. It can be concluded that the sorption mechanism may be a combination of electrostatic and physical sorption. At the start of the sorption process (i.e., chemical adsorption during the formation of a monolayer), ion exchange and Van der Waals interactions are predominantly responsible for the process.

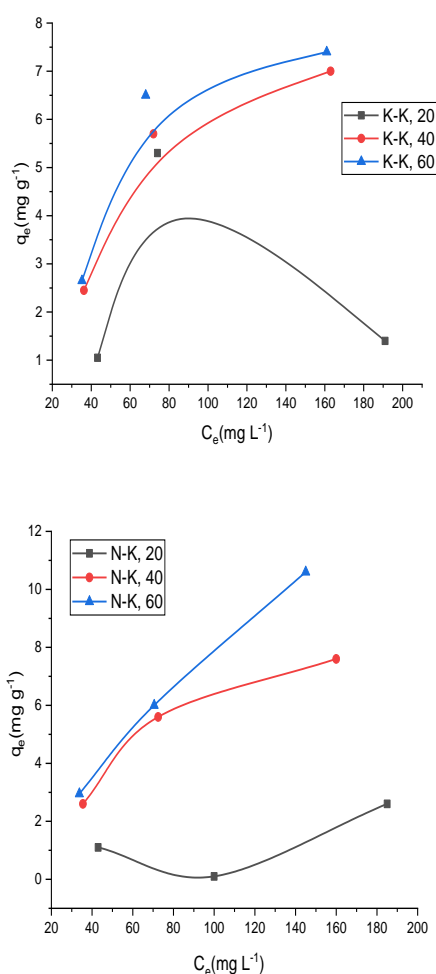


**Fig3.** Effect of temperature on the adsorption isotherms of K-K (up) and N-K (down) towards  $\text{Na}^+$ .

### 3.1.3. Effect of time of shaking

The effect of time of shaking on the adsorption of  $\text{Na}^+$  by the homo-ionized kaolin was investigated at an initial metal concentration of  $100 \text{ mg L}^{-1}$  within 10 – 1440 min shaking time (Fig. 4). It was observed that the metal ions removal by the K-K and N-

K increased with increasing the time of shaking to reach its equilibrium at 360 min yielding removal efficiencies of 15.0 and 36.3%, respectively.

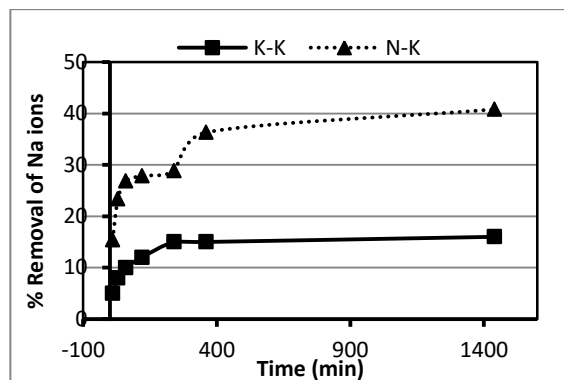


**Fig. 4** Effect of shaking time on the removal percentage of  $\text{Na}^+$  on K-K and N-K

This equilibration time is within the average values of reported results shown in Table (3), which is advantageous to guarantee a gradual release of exchanged nutrient ions to enable its beneficiation by the plant.

Adsorption kinetics of  $\text{Na}^+$  ions by homo-ionized kaolin were studied following the pseudo-first order, pseudo-second order and intraparticle diffusion models, described above. The characteristic parameters of pseudo-first-order and pseudo-second-order models are given in Table 4. These results show that the adsorption of  $\text{Na}^+$  ions on the homo-ionized kaolins is best described by pseudo-second order kinetic model with a high correlation coefficient (0.98-0.99), suggesting that the rate is limited by a chemisorption process, which is in accordance with the results obtained from adsorption isotherm models and thermodynamic studies. This supposes that the heterogeneous sorption mechanism may be responsible for the uptake of  $\text{Na}^+$  ions.

For intraparticle diffusion model, the adsorbate species may be transported from the bulk of the solution into the solid phase via intraparticle diffusion/transport processes, which are often the rate limiting step in many adsorption processes, especially in a rapidly stirred batch reactor<sup>[33]</sup>. This model was employed to identify the diffusion mechanism. The obtained values of  $C_i$  were 1.504 and 3.913  $\text{mg g}^{-1}$  for K-K and N-K, respectively that are related to the thickness of boundary layer. As  $C_i$  is not equal to zero, the adsorption processes is

rather complex and involves more than one diffusive resistance. The obtained results from this model showed low correlation coefficients, which indicates that this model does not describe the adsorption diffusion mechanism of Na<sup>+</sup> ions on the homo-ionized kaolin well. These results indicate that Na<sup>+</sup> ions slowly diffuse into the pores of the different adsorbents and therefore constitute a limiting step<sup>[34]</sup>.

**Table 4** Kinetic model constants and correlation coefficients for Na<sup>+</sup> adsorption on K-K and N-K.

Pseudo-first order				
Adsorbent	q <sub>e, exp</sub> (mg/g)	k <sub>1</sub>	q <sub>e, cal</sub> (mg/g)	R <sup>2</sup>
K-K	3.2	7.370 x 10 <sup>-3</sup>	1.940	0.9 <sup>γ</sup>
N-K	8.2	2.303 x 10 <sup>-3</sup>	4.365	0.8 <sup>γ</sup>
Pseudo-second order				
Adsorbent	H	k <sub>2</sub>	q <sub>e, cal</sub> (mg/g)	R <sup>2</sup>
K-K	0.102	9.424 x 10 <sup>-3</sup>	3.284	0.99
N-K	0.305	5.807 x 10 <sup>-3</sup>	7.245	0.9 <sup>α</sup>
Intraparticle diffusion				
Adsorbent	k <sub>ip</sub>	C <sub>i</sub>	R <sup>2</sup>	
K-K	0.057	1.504	0.67	
N-K	0.127	3.913	0.82	

## Conclusion

Natural kaolin clay of Egyptian origin was homo-ionized with K<sup>+</sup> and NH<sub>4</sub><sup>+</sup> to obtain K-K and N-K, respectively. K-K and N-K were successfully utilized as adsorbents for the simultaneous removal of Na<sup>+</sup> ions from aqueous solution and release of K<sup>+</sup> and NH<sub>4</sub><sup>+</sup> by batch adsorption method. The adsorption process was found to be dependent on initial concentration of Na<sup>+</sup> ions, contact time and temperature. The metal uptake increases with increasing the initial concentration probably due to the concomitant increase in kaolinitic volume and decrease in the dielectric constant. Optimum removal of metal ion was obtained at contact time of 360 min. The equilibrium data were best fitted with the Freundlich adsorption model. Pseudo-second order equation provided the best fit to the experimental data. The maximum capacities (q<sub>max</sub>) are found to be enhanced to 75.6 and 17.5 mg g<sup>-1</sup> for K-K and N-K, respectively. Thermodynamic analysis showed

that the process was spontaneous and thermodynamically favorable. Both homo-ionized kaolin samples are cheap adsorbents for decreasing the sodicity of soil

## 4. References

- 1 L. S. Sonon, U. Saha, D. Kissel, (2012). Agric. and Environm. Services Labo. The Univ. of Georgia
- 2 N. J. Warrence, J. W. Bauder, K. E. Pearson, (2002) Departement of Land Resources and Environmental Sciences, Montana State University-Bozeman, MT, 1-29.
- 3 P. Shrivastava, R. Kumar, (2015) Saudi journal of biological sciences, **22**, 123-131.
- 4 Y. H. Teow, A. W. Mohammad, (2019) Desalination, **451**, 2-17.
- 5 aA. S. K. Kumar, R. Ramachandran, S. Kalidhasan, V. Rajesh, N. Rajesh, (2012) Chemical Engineering Journal, **211**, 396-405; bM. A. D. Allah, A. A. Syed, 2018.
- 6 N. M. Alandis, W. Mekhamer, O. Aldayel, J. A. Hefne, M. Alam, (2019) Journal of Chemistry **2019**.
- 7 A. E.-M. MW, (2017), Nat Sci 15, 49-61.
- 8 T. Zhang, S. Wang, (2019) Materials, 12, 1671.
- 9 aR. A. Schoonheydt, C. T. Johnston, F. Bergaya, in Developments in Clay Science, Vol. 9, Elsevier, (2018), pp. 1-21; bR. M. Hazen, D. A. Sverjensky, D. Azzolini, D. L. Bish, S. C. Elmore, L. Hinnov, R. E. Milliken, American Mineralogist 2013, **98**, 2007-2029.
- 10 J. D. D. Moraes, S. R. A. Bertolino, S. L. Cuffini, D. F. Ducart, P. E. Bretzke, G. R. Leonardi, (2017) International journal of pharmaceutics, **534**, 213-219.
- 11 aB. Paul, J. J. Dynes, W. Chang, Desalination (2017), 419, 141-151; bE. Wibowo, M. Rokhmat, M. Abdullah, Desalination 2017, **409**, 146-156.
- 12 L. Liangxiong, T. M. Whitworth, R. Lee, (2003) Journal of Membrane Science, **217**, 215-225.
- 13 S. A. Drweesh, N. A. Fathy, M. A. Wahba, A. A. Hanna, A. I. M. Akarish, E. A. M. Elzahany, I. Y. El-Sherif, K. S. Abou-El-Sherbini, (2016), Journal of



- Environmental Chemical Engineering* **4**, 1674-1684.
- 14 N. P. Gibb, (2016).University of Saskatchewan
  - 15 A. I. Vogel, G. H. Jeffery, (1989).Vogel's textbook of quantitative chemical analysis, Wiley,
  - 16 I. Langmuir, (1918),*Journal of the American Chemical society* **40**, 1361-1403.
  - 17 H. Freundlich, (1906), *J. Phys. Chem* **57**, 1100-1107.
  - 18 M. Temkin, V. Pyzhev, (1940).
  - 19 Y. Liu, (2009) *Journal of Chemical & Engineering Data*, **54**, 1981-1985.
  - 20 S. Lagergren, (1898)*Handlingar*, **24**, 1-39.
  - 21 W. J. Weber, J. C. Morris, (1963) *Journal of the sanitary engineering division*, **89**, 31-60.
  - 22 aG. P. Robertson, P. Sollins, B. G. Ellis, K. Lajtha, (1999) Standard soil methods for long-term ecological research , 2, 462;bM. Kashem, B. Singh, T. Kondo, S. I. Huq, S. Kawai, *International Journal of Environmental Science & Technology* 2007, **4**, 169-176;cI.
  - 23 Snape, R. Scouller, S. Stark, J. Stark, M. Riddle, D. Gore, (2004) *Chemosphere*, **57**, 491-504.
  - 24 aC. Gianello, M. B. Amorim, *Communications in Soil Science and Plant Analysis* (2015), **46**, 94-103;bG. P. Robertson, D. C. Coleman, P. Sollins, C. S. Bledsoe, Standard soil methods for long-term ecological research, Vol. **2**, Oxford University Press on Demand, 1999.
  - 25 aC. H. Giles, D. Smith, A. Huitson, *Journal of colloid and interface science* 1974, **47**, 755-765;bC. H. Giles, A. P. D'Silva, I. A. Easton, (1974), *Journal of Colloid and Interface Science* **47**, 766-778.
  - 26 A. Sridharan, (2014) *Indian Geotechnical Journal*, **44**, 371-399.
  - 27 E. Hettiarachchi, R. Perera, A. Chandani Perera, N. Kottegoda, (2016)*Desalination and water treatment*, **57**, 22341-22352.
  - 28 D. Parmentier, M. Lavenas, E. Güler, S. J. Metz, M. C. Kroon, (2016)*Desalination*, **399**, 124-127.
  - 29 R. Rostamian, M. Heidarpour, S. Mousavi, M. Afyuni, (2015), *Journal of Agricultural Science and Technology* **17**, 1057-1069.
  - 30 A. M. Siemens, J. J. Dynes, W. Chang, (2020),*Environmental Technology* 1-12.
  - 31 M. Fathy, M. A. Mousa, T. A. Moghny, A. E. Awadallah, (2017),*Applied Water Science* **7**, 4427-4435.
  - 32 X. Wang, O. Ozdemir, M. A. Hampton, A. V. Nguyen, D. D. Do, (2012), *Water Research* **46**, 5247-5254.
  - 33 O. Santiago, K. Walsh, B. Kele, E. Gardner, (2016) ,*J. Chapman, SpringerPlus* **5**, 571.
  - 34 S. A. Drweesh, N. A. Fathy, M. A. Wahba, A. A. Hanna, A. I. Akarish, E. A. Elzahany, I. Y. El-Sherif, K. S. Abou-El-Sherbini, (2016),*Journal of Environmental Chemical Engineering* **4**, 1674-1684.
  - 35 J. N. Ghogomu, T. D. Noufame, M. J. Ketcha, N. J. Ndi, (2013), *British Journal of Applied Science & Technology* **3**, 942-961.